Drug Design, Development and Therapy

Dovepress
Taylor & Francis Group

Open Access Full Text Article

ORIGINAL RESEARCH

Exploring the Anti-PANoptosis Mechanism of Dachaihu Decoction Against Sepsis-Induced Acute Lung Injury: Network Pharmacology, Bioinformatics, and Experimental Validation

Zhen Yang[1,2], Xingyu Kao[1,2], Lin Zhang[3], Na Huang[1,2], Jingli Chen[2], Mingfeng He[2]

[1]The Eighth Clinical Medical College of Guangzhou University of Chinese Medicine, Foshan, Guangdong, People's Republic of China; [2]Foshan Hospital of Traditional Chinese Medicine, Foshan, Guangdong, People's Republic of China; [3]Department of Cardiovascular, Integrated Hospital of Traditional Chinese Medicine, Southern Medical University, Guangzhou, People's Republic of China

Correspondence: Mingfeng He, Foshan Hospital of Traditional Chinese Medicine, Foshan, Guangdong, People's Republic of China, Email he-mingfeng@foxmail.com

Background: Dachaihu decoction (DCHD) is a common Chinese medicine formula against sepsis-induced acute lung injury (SALI). PANoptosis is a novel type of programmed cell death. Nevertheless, The mechanisms of DCHD against SALI via anti-PANoptosis remains unknown.

Methods: First, we identified the intersecting targets among DCHD, SALI, and PANoptosis using relevant databases and published literature. Then, protein-protein interaction (PPI) network, molecular docking, and functional enrichment analysis were conducted. In vivo, cecal ligation and puncture (CLP) was used to construct a sepsis mouse model, and the therapeutic effects of DCHD on SALI were evaluated using hematoxylin and eosin (H&E) staining, quantitative real-time PCR (qRT-PCR), and ELISA. Finally, qRT-PCR, immunofluorescence staining, and Western blotting were used to verify the effect of DCHD-containing serum (DCHD-DS) on LPS-induced RAW 264.7 macrophages in vitro.

Results: 82 intersecting targets were identified by mapping the targets of DCHD, SALI, and PANoptosis. Enrichment analysis showed that DCHD against SALI via anti-PANoptosis by modulating tumor necrosis factor (TNF), AGE-RAGE, phosphoinositide 3-kinase (PI3K)-AKT, and Toll-like receptor signaling pathways by targeting Casp3, cellular tumor antigen p53 (TP53), B-cell lymphoma 2 (Bcl2), toll-like receptor-4 (TLR4), STAT3, STAT1, RELA, NF-κB1, myeloid cell leukemia-1 (MCL1), JUN, IL-1β, HSP90AA1, Casp9, Casp8, and Bcl2l1. Molecular docking analysis revealed that the key components of DCHD have a high binding affinity to the core targets. In vivo, DCHD improved lung histopathological injury, reduced inflammatory factor expression, and alleviated oxidative stress injury in lung tissues. In vitro, DCHD-DS alleviated cell morphology changes, the release of pro-inflammatory factors, and p65 nucleus aggregation. Furthermore, we verified that DCHD-DS inhibited PANoptosis by downregulating the PI3K/AKT/NF-κB signalling pathway.

Conclusion: DCHD attenuates SALI by inhibiting PANoptosis via control of the PI3K/AKT/NF-κB pathway. Our study provides a solid foundation for investigating the mechanisms of DCHD and its clinical application in the treatment of SALI.

Keywords: Dachaihu decoction, sepsis-induced acute lung injury, PANoptosis, network pharmacology, bioinformatics

Introduction

Sepsis is a dysregulated response to infection that occurs when the host resists pathogen invasion, causing a life-threatening systemic inflammatory response and triggering immune suppression and organ dysfunction, ultimately leading to multiple organ failure and mortality.[1,2] The lungs are connected to the external environment and are the most vulnerable and susceptible organ to sepsis.[3] Acute lung injury (ALI) is a common and serious complication of sepsis, is closely associated with high morbidity and mortality in septic patients,[4] often further aggravated to acute

Received: 17 October 2024
Accepted: 31 December 2024
Published: 17 January 2025

© 2025 Yang et al. This work is published and licensed by Dove Medical Press Limited. The full terms of this license are available at https://www.dovepress.com/terms.php and incorporate the Creative Commons Attribution – Non Commercial (unported, v3.0) License (http://creativecommons.org/licenses/by-nc/3.0/). By accessing the work you hereby accept the Terms. Non-commercial uses of the work are permitted without any further permission from Dove Medical Press Limited, provided the work is properly attributed. For permission for commercial use of this work, please see paragraphs 4.2 and 5 of our Terms (https://www.dovepress.com/terms.php).

Graphical Abstract

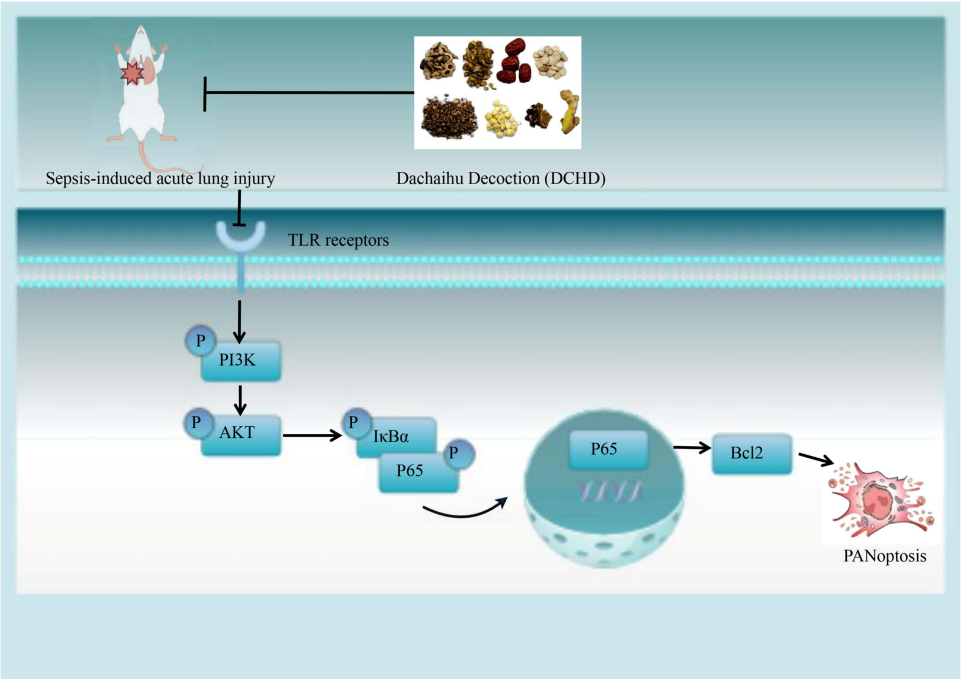

respiratory distress syndrome (ARDS).[5] According to an epidemiological survey in China, the prevalence of ALI in patients with sepsis is approximately 68.2% and the 90-day mortality rate in patients with ALI is approximately 35.5%.[6] Alveolar epithelium and vascular endothelium injury, increased alveolar capillary permeability, and decreased alveolar surfactant levels are important pathological processes in sepsis-induced acute lung injury (SALI).[7,8] Nuclear factor kappa-B (NF-κB), janus kinase (JAK)/signal transducer and activator of transcription (STAT), mitogen-activated protein kinase (MAPK), and Notch signaling pathways are thought to be associated with alveolar injury and repair in SALI.[9] However, the pathogenesis of SALI remains unknown and effective treatment is still lacking at present.

With increasing research on SALI, many programmed cell death processes including autophagy, apoptosis, necrosis, and pyroptosis have been found to be closely related to its pathogenesis.[10] Notably, PANoptosis is a recently proposed approach for programmed inflammatory cell death regulated by the PANoptosome, the key features of which are pyroptosis, apoptosis, and necroptosis.[11] It has been found that infection, cytokine storm and cancer stimulation often induce PANoptosis, and thus the progression of diseases such as infection, inflammatory diseases, cancer and neurodegenerative diseases is closely related to PANoptosis.[12,13] Moreover, Recent studies have shown that PANoptosis plays a pivotal role in ALI. It was demonstrated recently that ursodeoxycholic acid attenuates SALI by inhibiting PANoptosis-like cell death through the STING pathway.[14] It was reported that miR-29a-3p could inhibit PANoptosis and inflammation in alveolar epithelial cells and ameliorate LPS-induced ALI by targeting TNFR1.[15] Our previous study confirmed that interleukin (IL)-1β, factor-related apoptosis (FAS), and cluster of differentiation (CD) 14 may be critical targets in PANoptosis and are involved in the progression of SALI.

Traditional Chinese medicine (TCM) has a long history of treating infectious diseases and unique advantages in treating SALI. Recent research has revealed that Lianhua Qingwen,[16] Wenqingyin,[17] QiShenYiQi pills,[18] Xuebijing,[19] Jinhong decoction[20] and other Chinese medicinal preparations can improve SALI through anti-inflammatory effects and attenuate pulmonary vascular barrier damage. Dachaihu decoction (DCHD) originally derived from "Treatise on Febrile Diseases", written by Zhang Zhongjing in the Eastern Han Dynasty. DCHD consists of eight herbs, namely, *Bupleurum chinense* DC. (Chaihu), *Scutellaria baicalensis* Georgi (Huangqin), *Pinellia ternata* Breit. (Banxia), *Citrus aurantium*

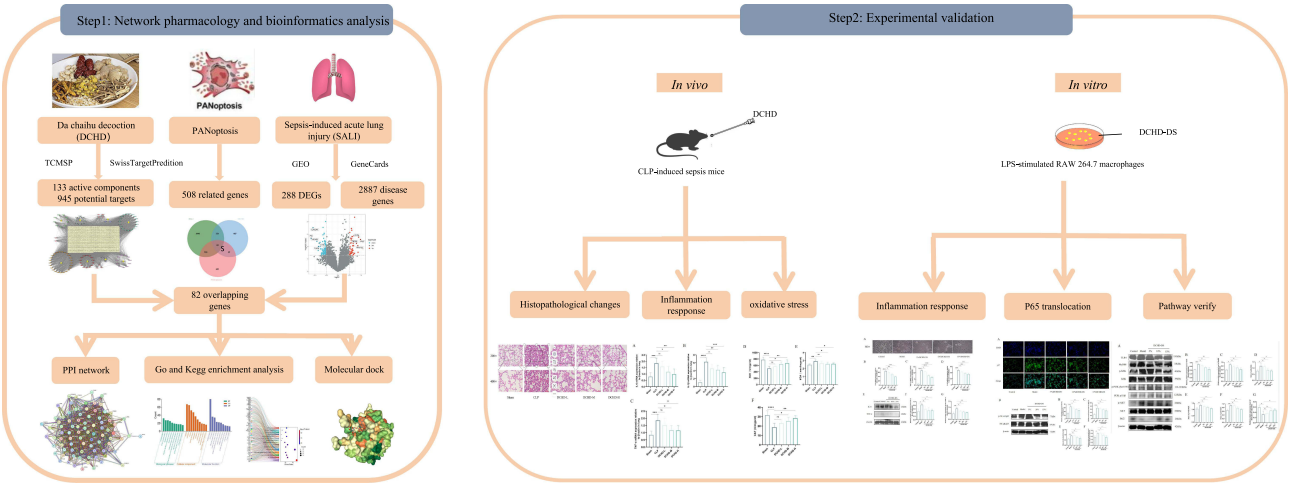

Figure 1 The flowchart of the research.

L. (Zhishi), *Rheum officinale* Baill. (Dahuang) and *Zingiber officinale* Roscoe. (Shengjiang), *Paeonia lactiflora* Pall. (Shaoyao), *Ziziphus jujuba* Mill. (Dazao), with equivalent ratios. DCHD exerts the effects of "reconcilng Shaoyang and clearing Yang Ming evil heat", and Yangming is linked to the spleen, stomach, lung, and large intestine based on the TCM theory. Besides, according to the theory of "lung and large intestine stand in exterior-interior relationship", DCHD can treat lung-related diseases. DCHD has documented anti-inflammatory,[21] regulation of the intestinal flora,[22] and inhibition of macrophage infiltration.[23]

Network pharmacology is one of the frontiers and hotspots in the field of TCM research, assessing the biological network mechanisms between Chinese herbs and diseases through multi-component and multi-target regulatory networks. Bioinformatics is widely used for various genomic analyses including transcriptomics, genomics, and epigenetics. Bioinformatic analysis combined with microarray technology can explore molecular mechanisms and develop effective treatments for a variety of diseases through a comprehensive investigation of potential novel biomarkers and their functions.[24] In order to investigate the regulatory mechanism of DCHD on PANoptosis in SALI, bioinformatics analysis was employed to identify the differentially expressed genes (DEGs) of SALI, and the network pharmacology approach was used to identify the DCHD target network and reveal the pathway of DCHD against SALI by inhibiting PANoptosis via control of the PI3K/AKT/NF-κB pathway. Finally, we verified the results in vitro and in vivo, intending to provide new insights for the treatment of SALI. The specific research process is shown in the flowchart (Figure 1).

Materials and Methods

Materials

Superoxide dismutase (SOD), malondialdehyde (MDA), and catalase (CAT) were obtained from Nanjing Jiancheng Bioengineering Institute (Nanjing, China). The PrimeScript™ RT Master Mix Kit and SYBR Green I™ Premix Ex Taq PT™ kits were purchased from Takara Biomedical Technology Co., Ltd.(Beijing, China). RIPA lysis buffer, TRIzol, DAPI, anti-fade mounting medium, protease and phosphatase inhibitors, bovine serum albumin (BSA), loading buffer, ECL Substrate Kit and BCA protein assay kit were purchased from Beyotime Biotechnology (Shanghai, China). Primary antibodies to toll-like receptor-4 (TLR4; 66350-1-lg), myeloiddifferentiationfactor88 (MyD88; 67969-1-lg), inhibitor kappa B alpha (IκBα; 66418-1-lg), NF-κB p65 (80979-1-RR), Phospho-NF-κB p65 (82335-1-RR), protein kinase B (AKT) (60203-2-Ig), Phospho-AKT (29163-1-AP), B-cell lymphoma 2 (Bcl2) (66799-1-Ig), β-actin (81115-1-RR), HRP-conjugated Affinipure Goat Anti-Mouse IgG (H+L) (SA00001-1), HRP-conjugated Affinipure Goat Anti-Rabbit IgG (H+L) (SA00001-2) and CoraLite488-conjugated Goat Anti-Rabbit IgG(H+L) (SA00013-2) secondary antibodies were purchased from Proteintech (Chicago, IL, USA). Phosphoinositide 3-kinase (PI3K) p110β (HY-P81229) and phospho-PI3K p110β (Ser1070) (HY-P81211) were purchased from MedChemExpress (New Jersey, USA). Interleukin

https://doi.org/10.2147/DDDT.S495225

(IL)-6 (YP-Ab-16022) and tumor necrosis factor (TNF)-α (YP-Ab-15972) were purchased from UpingBio (Hangzhou, China). Dulbecco's modified Eagle's medium (DMEM) and fetal bovine serum (FBS) were purchased from GIBCO BRL (Grand Island, NY, USA). Penicillin-streptomycin (P/S) solution was obtained from Pricella Biotechnology Co. Ltd. (Wuhan, China). LPS (L2880, 055:B5) was obtained from Sigma-Aldrich (St. Louis, MO, USA).

DCHD Preparation and Quality Control

Beijing Kangmei Pharmaceutical Co. Ltd. (Beijing, China) provided all DCHD. The DCHD consists of eight herbs: Chaihu 15 g, Huangqin 9 g, Banxia 9 g, Zhishi 9 g, Dahuang 6 g, Shaoyao 9 g, Shengjiang 15 g, Dazao 12 g. DCHD was prepared as previously described.[25] Briefly, the gavage dose for mice was calculated based on an adult body weight of 70 kg and an equivalent dose ratio of 0.026 between human and mouse body surface area.[26] 84 g crude herbs of DCHD were soaked in distilled water for 30 min and boiled twice with 12-fold or 10-fold distilled water for 1 h each time. The two herbal solutions were mixed, filtered, and boiled for another 30 min, then filtered, distilled, and concentrated to 1 g/mL crude drug and stored at 4 °C for subsequent use. The constituents of DCHD were identified using high-performance liquid chromatography combined with mass spectrometry (HPLC-MS) for quality control and to create a characteristic fingerprint in the previous study[22] (Supplementary Tables S1, S2 and Figure S1).

Identification of the Active Components and Potential Targets of DCHD

The Traditional Chinese Medicine Systems Pharmacology Database[27] (TCMSP, https://tcmspw.com/tcmsp.Php) was used to filter out the activecomponents of DCHD as determined by the criteria for absorption, distribution, metabolism, and excretion (ADME) (oral bioavailability ≥ 30% and drug-likeness ≥ 0.18).[28] SMILES structures of the active components were confirmed using the PubChem database (https://PubChem.ncbi.nlm.nih.gov).[29] Then, the SMILES structures were imported into the SwissTargetPrediction (http://www.swisstargetprediction.ch/),[30] specifying "Homo sapiens", to predict all potential targets of the active components in DCHD. All the active components of DCHD and their corresponding potential targets were imported into Cytoscape3.7.0 to construct the "DCHD-active component-target" network.

Identification of Disease Gene Targets and PANoptosis-Related Genes

Disease-related targets were searched using GeneCards (https://www.genecards.org/) and the NCBI Gene Expression Omnibus[31] (GEO; https://www.ncbi.nlm.nih.gov/geo/). Specifically, "sepsis" and "acute lung injury" were used as key terms in the search for gene sets in the GeneCards database. The sequencing data for GSE10474, GSE32707, and GSE66890 were downloaded from the GEO database. To filter DEGs from the three integrated datasets, the LIMMA package was used with a P-value < 0.05 and |log2 fold-change (FC)|≥0.5 as screening criteria. The results collected from the two databases were combined to identify the disease targets for SALI. Furthermore, we searched for PANoptosis-related genes in the published literature,[32,33] and PANoptosis-related genes were identified by merging gene sets and removing duplicate genes. Finally, using the jvenn platform[34] (https://jvenn.toulouse.inrae.fr/app/example.html), the predicted targets of DCHD, disease targets, and PANoptosis-related genes were selected to identify the targets of DCHD for the treatment of SALI via anti-PANoptosis.

Construction of Protein-Protein Interaction (PPI) Network and Identification of Hub Genes

The intersection targets obtained in the previous step were imported into the STRING database (version 11.5, https://cn.string-db.org/) to construct the PPI network and the minimum required interaction score was set to medium confidence (0.400). The TSV file downloaded from the STRING database was then inputted into Cytoscape 3.7.0, and the CytoHubba plugin was used to screen the top 15 core genes ranked by Maximal Clique Centrality (MCC) as hub genes.

Gene Function and Pathway Enrichment Analysis

Gene Ontology (GO) and Kyoto Encyclopedia of Genes and Genomes (KEGG) pathway enrichment analysis were performed using DAVID database (https://david.abcc.ncifcrf.gov/). GO analysis typically describes three aspects of gene

function: biological pathways (BP), cellular components (CC), and molecular functions (MF). KEGG pathway enrichment analysis revealed the crucial signaling pathways of DCHD in the treatment of SALI via anti-PANoptosis. A bioinformatics platform (https://www.bioinformatics.com.cn/) was used for data analysis and visualization.

Molecular Docking Analysis

Molecular docking is a computer simulation of the intermolecular recognition process to predict the binding mode and binding strength and is often used for disease mechanism research and new drug development.[35] Small-molecule ligands were downloaded from PubChem (https://pubchem.ncbi.nlm.nih.gov/) and the 3D structures of the protein receptors were downloaded from the RCSB PDB (http://www.rcsb.org/). Subsequently, the structures of the proteins and ligands were preprocessed, including the removal of water molecules and ions and the addition of hydrogen atoms. Molecular docking and visualization of ligands and protein receptors were performed using Auto Dock Tools 1.5.6 and Py MOL 2.3.4. It is generally recognized that binding energies < −4.25 kcal/mol indicates good ligand-receptor affinity, and < −7 kcal/mol is regarded as having strong docking affinity.[36]

Animal Model and Animal Group

Guangzhou Regal Biotechnology Co., Ltd., provided C57BL/6 mice (male, 6-8-weeks old, weighting 20–22 g). Our research was conducted according to the International Ethics Guidelines and the National Institutes of Health Guidelines Concerning the Care and Use of Laboratory Animals. All animal experimental procedures were approved by the Laboratory Animal Welfare and Ethics Committee of the School of Pharmaceutical Sciences, Guangzhou University of Chinese Medicine (No. ZYD-2023-101, No. ZYD-2023-102).

Cecal ligation and puncture (CLP) method was used to construct a sepsis mouse model.[37] Briefly, mice were anesthetized with an intraperitoneal injection of 1% pentobarbital (0.08 mL/10 g). The cecum was exposed after opening the abdominal cavity of the mice. The distal end of the ileocecal valve of the cecum was ligated using a 4–0 silk thread and punctured twice using a 21G puncture needle. The cecum was then returned to the abdominal cavity after gently squeezing a small amount of feces. For a parallel study, mice in the sham group were only opened abdominal cavity to expose the cecum, and then the abdominal cavity was sutured in the absence of CLP. Subsequently, 0.9% saline (37°C, 0.5 mL/10 g) was used for subcutaneous injection, and all mice were placed on the animal insulation blanket until resuscitation. All surgeries were performed by a single operator to minimize errors in our experiments.

Five groups were randomly assigned: sham group (n=10); CLP group (n=14); and DCHD-H, -M, and-L groups (n=12). The methods of gavage and drug administration have been described in our previous research.[25] Briefly, the mice in the DCHD-L, DCHD-M, and DCHD-H treatment groups were exposed to different concentrations of DCHD (5.46, 10.92, and 21.84 g/kg/d, respectively) by gavage. In contrast, the mice in the CLP and sham groups were exposed to an equivalent volume of saline. All mice were sacrificed 24 h after surgery and blood and lung tissue samples were collected.

DCHD Drug Containing Serum (DCHD-DS) Preparation

After three days of acclimatization, 20 male Sprague-Dawley rats (weighing 200 ± 20 g) were randomly divided into two groups: control group (n=8) and DCHD-DS group (n=12). Rats in the DCHD-DS group were administered DCHD (7.56 g/kg/d) by gavage twice a day at 12-h intervals, whereas rats in the control group were gavaged with an equal amount of saline. After the last gavage on the 3th day, all rats were anesthetized, blood was collected via the abdominal aorta, and after standing at room temperature for 2 h, serum was obtained by centrifugation at 4000 rpm for 15 min and dispensed into sterile EP tubes in a sterile environment. After being inactivation for 30 min at 56 °C in a water bath, the blood samples were filtered through a 0.22μm microporous membrane to remove impurities and bacteria, and then stored at −80 °C.[38]

RAW 264.7 Cells Culture and Treatment

RAW 264.7 cells were purchased from the Cell Bank of the Chinese Academy of Sciences (Shanghai, China). Cells were cultured in DMEM containing 10% FBS and 1% P/S at 37 °C in a humidified incubator with a 5% CO_2 atmosphere. To investigate the effect of DCHD-DS on LPS-induced RAW 264.7 macrophages, the cells were exposed to different concentrations of DCHD-DS (5%, 10%, and 15%) cells for 1h, and then 1ug/mL LPS was added to the medium for another 12 h.[17] The cells were divided into five groups: control group, model group (1ug/mL LPS), and DCHD-DS (5%, 10%, and 15% + 1ug/mL LPS) groups.

Histopathological Analysis

Fresh lung tissue samples were soaked in 4% paraformaldehyde (PFA), fixed for 24 h, dehydrated using gradient ethanol, paraffin-embedded, and sliced into 4-μm-thick slices using a sectioning machine for hematoxylin and eosin (H&E) staining. The lung injury score refers to previously published scoring criteria and consists of four main aspects: inflammatory infiltrates, interstitial edema, alveolar edema, and alveolar hemorrhage, with a score of 0–4 for each item. The higher the severity, the higher the score, and the higher the total score, the more severe the lung injury.[39]

Biochemical Analysis

We weighed 100 mg of tissue and added 900 μL of saline to homogenize in a homogenizer to obtain 10% lung tissue homogenate by centrifugation 10 min at 3000 rpm at 4 °C. SOD, MDA, and CAT levels in lung tissues were determined using the corresponding assay kits.

Immunofluorescence Staining

After the cells were plated and treated, the culture medium was removed, and the cell-climbing sections were fixed with 4% paraformaldehyde for 20 min and permeabilized with 0.1% TritonX-100. Sections were blocked with 3% BSA for 30 min at room temperature with primary antibodies was incubated at 4 °C overnight. After incubation with the fluorescent secondary antibody for 1 h at room temperature, the slides were stained with DAPI for 5 min in the dark. The slices were then sealed with an anti-fade mounting medium and fluorescence microscopy was used for observation and image acquisition.

RNA Extraction and Quantitative Real-Time PCR (qRT-PCR)

Total RNA was extracted from lung tissues and RAW 264.7 cells using TRIzol reagent, and the purity and concentration of total RNA were determined using an enzyme-labeling instrument (BioTek Epoch 2, Vermont, USA). Subsequently, the mRNA was reverse-transcribed into cDNA following the instructions of the PrimeScript™ RT Master Mix Kit (37°C for 15 min, 85°C for 5s, and stored at 4 °C). The mRNA expression levels were determined using the SYBR Green I™ Premix Ex Taq PT™ kits on an Applied Biosystems® 7500 Fast Real-Time PCR System (Applied Biosystems Inc., Carlsbad, CA, USA), followed by 95 °C for 30s, 95 °C for 5s, 60 °C for 34s, for 40 cycles. The relative mRNA levels were calculated using the $2^{-\Delta\Delta CT}$ approach, and β-actin was used as a control. Primer sequences were synthesized by Shanghai Shenggong Technology Co., Ltd. Table 1 presented the primer sequences.

Table 1 Primer Sequence

Gene	F	R
TNF-α	CCTGTAGCCCACGTCGTAG	GGGAGTAGACAAGGTACAACCC
IL-1β	GAAATGCCACCTTTTGACAGTG	TGGATGCTCTCATCAGGACAG
IL-6	TAGTCCTTCCTACCCCAATTTCC	TTGGTCCTTAGCCACTCCTTC
β-actin	GTGACGTTGACATCCGTAAAGA	GCCGGACTCATCGTACTCC

Abbreviations: TNF-α, tumor necrosis factor-α; IL-1β, Interleukin-1β; IL-6, Interleukin-6.

Western Blot Assays

Total proteins were extracted from lung tissues and RAW 264.7, using RIPA lysis buffer containing 1 mm protease and phosphatase inhibitors. The protein concentration of the samples was determined according to the BCA protein assay kit instructions, and different doses of 5 × loading buffer and RIPA buffer were added to normalize the protein concentrations. The protein samples were separated using 6%, 10%, and 10% sodium dodecyl sulfate-polyacrylamide gel electrophoresis (SDS-PAGE) based on protein molecular weight. Then, the gels were transferred to 0.45μm or 0.22μm polyvinylidene fluoride (PVDF) membranes. We used 2% milk powder solution to blocked the membranes for 1 h at room temperature, then primary antibodies were added and incubated overnight at 4 °C, including TLR4 (mouse, 1:1000), Myd88 (mouse, 1:1000), IκBα (mouse, 1:2000), NF-κB p65 (rabbit, 1:1000), p-IκBα (rabbit, 1:500), p-NF-κB p65 (rabbit, 1:1000), PI3K (rabbit, 1:1000), p-PI3K (rabbit, 1:1000), AKT (rabbit, 1:1000), p-AKT (rabbit, 1:1000), Bcl2 (mouse, 1:1000), IL-6 (rabbit, 1:1000), TNF-α (rabbit, 1:1000). In addition, the blots were incubated with anti-mouse or anti-rabbit IgG HRP-labeled secondary antibodies at room temperature for 1 h. Finally, the protein blots were detected using an enhanced chemiluminescence detection system (Bio-Rad, Hercules, California, USA) with the addition of an ECL Substrate Kit. The protein bands on the blots were analyzed using ImageJ software and normalized to the β-actin protein levels.

Statistical Analysis

The sample size in our experiments was 5–6 independent observations per experimental group. GraphPad Prism 9.5.0 (GraphPad Software, San Diego, CA, USA) was used for the statistical analyses and figures construction. Data are presented as mean ± SD. For the analysis of significant difference between multiple groups, we first performed normality test and homogeneity of variance test, if the data conformed to normal distribution and homogeneity of variance, the one-way analysis of variance (ANOVA) test was used; if it did not conform to normal distribution, the Kruskal–Wallis non-parametric test was selected; if it conformed to normal distribution but the heterogeneity of variance, the Welch test was used. Statistical significance was set at $P < 0.05$.

Results

Active Components and Targets Prediction of DCHD

A total of 151 active components of DCHD were identified in the TCMSP database, including 17 from Chaihu, 36 from Huangqin, 16 from Dahuang, 22 from Zhishi, 13 from Banxia, 13 from Shaoyao, five from Shengjiang, and 29 from Dazao. After removing duplicates, 133 active components containing 33 components with unidentified SMILES structures were obtained from the PubChem database (Supplementary Tables S3 and S4). Subsequently, 945 potential targets were predicted using SwissTargetPrediction after the deletion of duplicates. The "DCHD-active component-target" network was constructed through Cytoscape3.7.0 (Figure 2).

Identification of the Targets of SALI and PANoptosis Gene Set

Using the keywords "sepsis" and "acute lung injury", 2887 SALI-related targets were obtained from GeneCards. The microarray datasets GSE10474, GSE32707, and GSE66890 contained 79 control group samples and 60 SALI group samples from the GEO database, and a box plot was used to normalize these samples (Figure 3A). A total of 288 DEGs were screened under the criteria of p-value < 0.05 and $|\log2FC| \geqq 0.5$, with 107 upregulated genes and 181 downregulated genes, and the heat map and volcano plot of differential expression analysis are presented (Figure 3B and C). Therefore, 3089 target genes of SALI were identified after removing duplicates. We also collected 508 PANoptosis-related genes from the published literature (Figure 3D).

Construction of the Venn Diagram and PPI Network

To obtain the intersecting targets of DCHD against SALI via anti-PANoptosis, 82 intersecting targets were identified by mapping the targets of DCHD-, SALI-, and PANoptosis-related genes using the jvenn platform (Figure 4A). Subsequently, 82 common targets were imported into the STRING database to obtain the "TSV" file and a PPI network

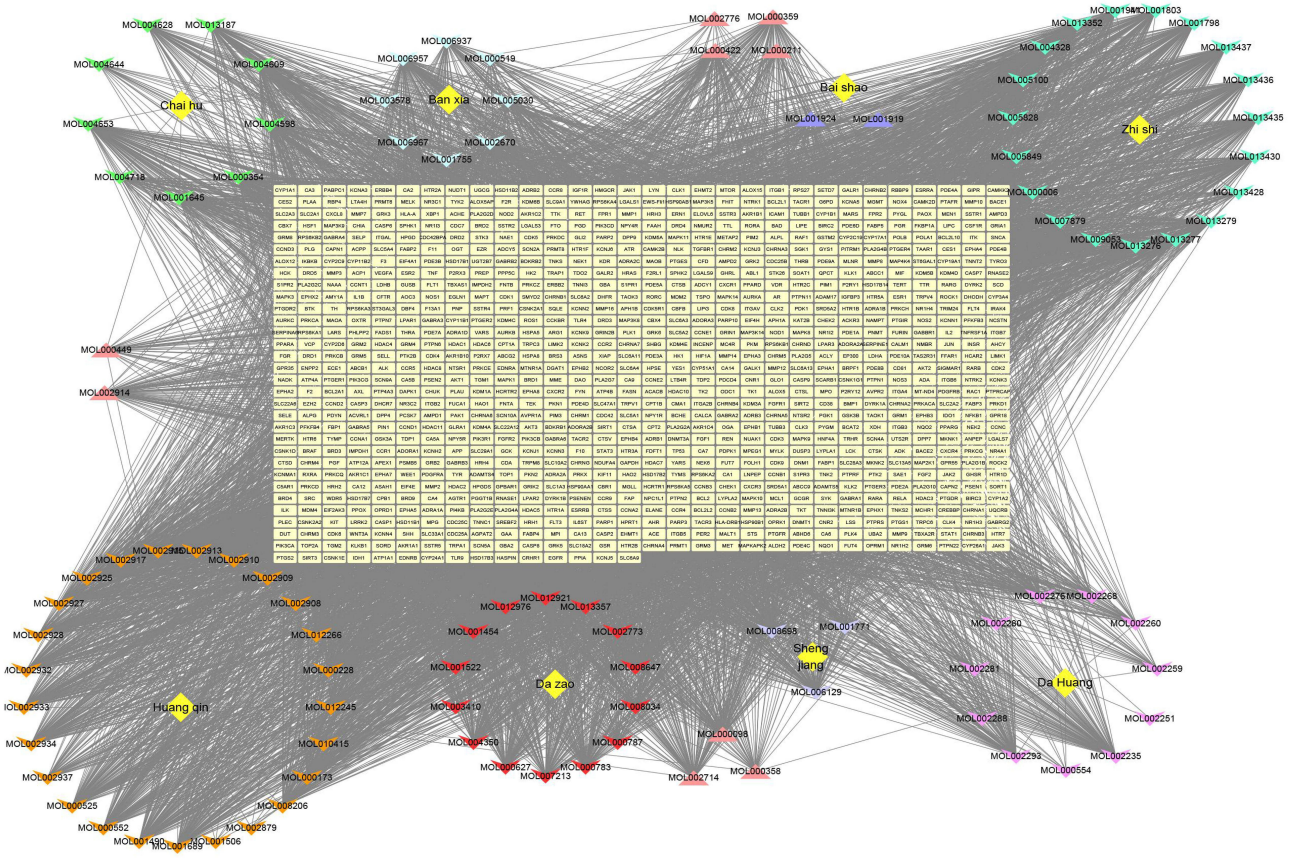

Figure 2 Chinese herbs-Components-Targets network diagram. The yellow diamond-shaped nodes represent Chinese herbs in DCHD, and different colors of shuttle nodes correspond to different herbal components. The triangular nodes represent shared components, and the yellow square nodes represent drug targets. The connection lines represent the relationship between them.

was constructed with 79 nodes and 1314 edges using Cytoscape 3.7.0 software (Figure 4B and C). The CytoHubba plugin in Cytoscape was used with MCC to screen for hub genes (Figure 4D) including caspase (Casp)-3, cellular tumor antigen p53 (TP53), Bcl2, TLR4, Signal Transducer And Activator Of Transcription (STAT)-3, STAT1, NF-κB p65 (RELA), p50 (NF-κB1), myeloid cell leukemia-1 (MCL1), JUN, IL-1β, Heat shock protein (HSP)-90AA1, Casp9, Casp8, and Bcl2l1. The details of the hub genes are shown in Table 2.

GO and KEGG Functional Enrichment Analysis

To perform GO and KEGG pathway enrichment analysis, 82 common targets were imported into the DAVID database to identify biological processes and enriched pathways. We identified the top 10 items of BP, CC, and MF separately in GO analysis, and they were primarily involved in the underlying molecular functions, cellular location, and biological processes. BP is primarily involved in phosphorylation, protein phosphorylation, and apoptosis. CC primarily involves the cytosol, cytoplasm, and the nucleus. MF mainly comprised of protein binding, ATP binding, and identical protein binding (Figure 4E). Therefore, the various abnormal biological processes described above are thought to participate in the development of SALI, and DCHD may play a protective role in SALI by modulating the biological processes involved in anti-PANoptosis. KEGG pathway enrichment analysis identified the critical signaling pathways of DCHD against SALI by anti-PANoptosis, including apoptosis, TNF signaling pathway, C-type lectin receptor signaling pathway, AGE-RAGE signaling pathway in diabetic complications, PI3K-AKT signaling pathway, neurotrophin signaling pathway, Necroptosis, and Toll-like receptor signaling pathway (Figure 4F). Previous studies have revealed that the PI3K-AKT and Toll-like receptor signaling pathways are closely related to inflammation, PANoptosis,[40,41] and pulmonary

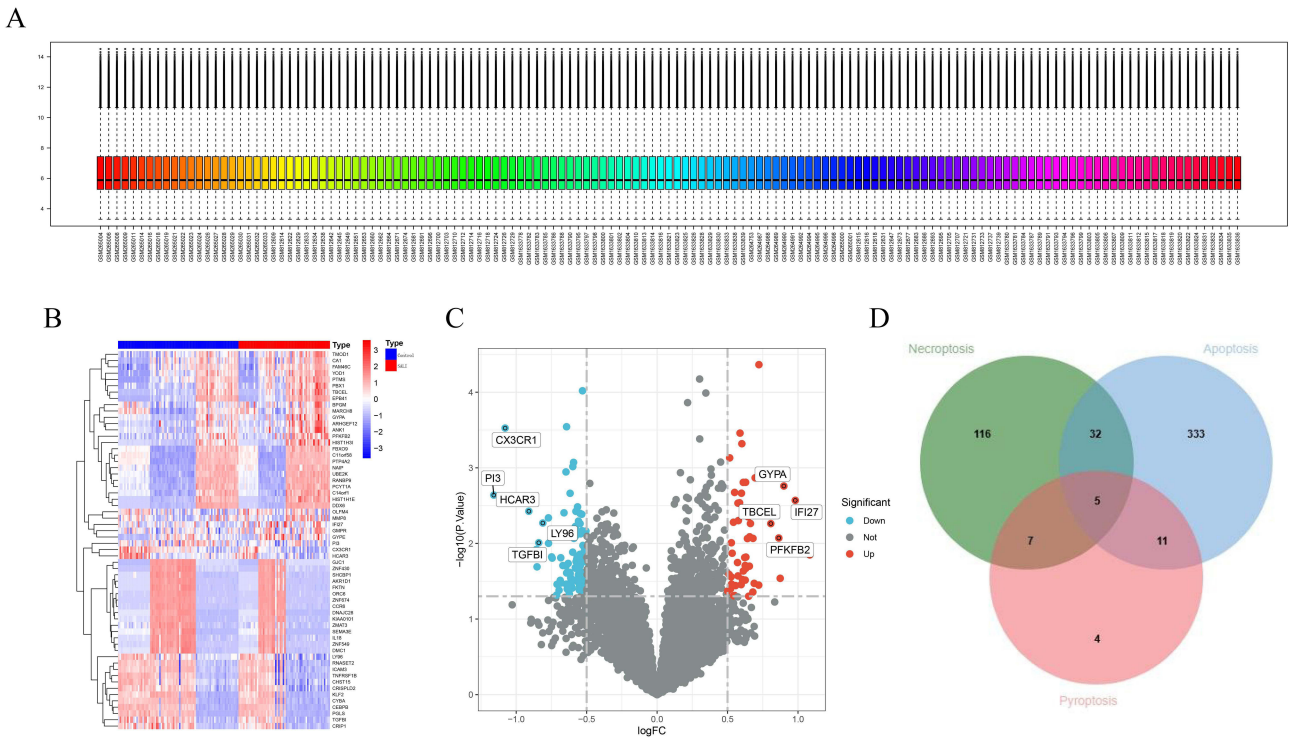

Figure 3 Identification of DEGs of SALI and PANoptosis related genes. (**A**) Boxplot of raw data normalized between samples. (**B**) Heat map of DEGs. Blue and red represent the low and highly expressed DEGs in the samples, respectively. (**C**) Volcano plot of DEGs. Red and green represent up and down regulated DEGs, respectively, grey represents no significant difference. (**D**) The Venn diagram of PANoptosis gene set consisting of pyroptosis, apoptosis and necroptosis.

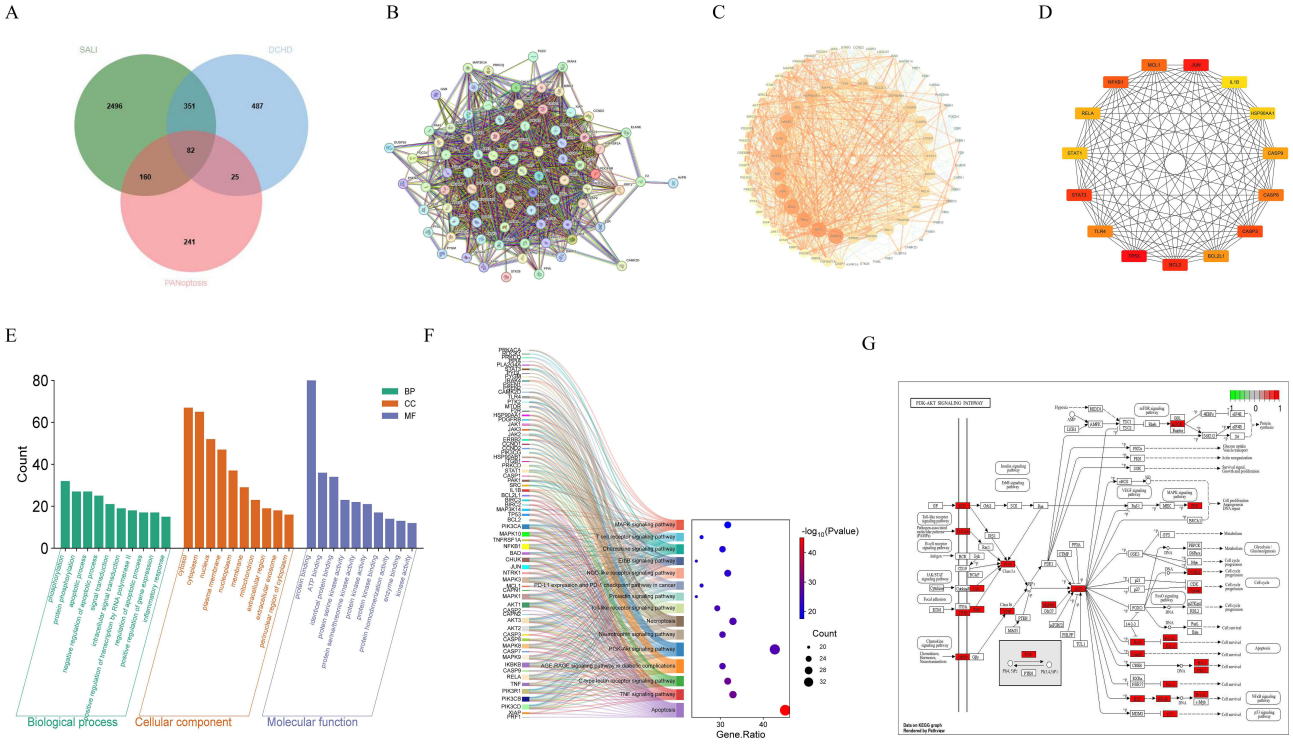

Figure 4 PPI network, GO and KEGG enrichment analysis. (**A**) Venn diagram of the intersection of DCHD, SALI, and PANoptosis. (**B** and **C**) PPI network analysis among the intersection targets through STRING database and Cytoscape 3.7.0 software. The nodes in the figure have larger size, deeper colors and thicker connecting lines indicating greater significance. (**D**) Hub gene identified by CytoHubba plugin-in of Cytoscape with MCC. (**E**) Top 10 BP, CC and MF terms by GO enrichment analysis. (**F**) Sankey and dot plot of top 15 KEGG enrichment pathways. (**G**) The distribution of core genes in the PI3K/AKT/NF-κB pathway.

https://doi.org/10.2147/DDDT.S495225

Table 2 Details of the Hub Genes

No.	Gene	Degree	Betweenness Centrality	Closeness Centrality
1	Casp3	67	0.06411242	0.84375
2	TP53	64	0.0250351	0.81818182
3	Bcl2	64	0.02818422	0.81818182
4	TLR4	51	0.00936788	0.72321429
5	STAT3	59	0.01373577	0.77884615
6	STAT1	48	0.00956616	0.70434783
7	NF-κB p65 (RELA)	47	0.0134682	0.69827586
8	p50 (NF-κB1)	59	0.01687364	0.77884615
9	MCL1	46	0.00589036	0.69230769
10	JUN	63	0.03266881	0.81
11	IL-1β	59	0.03707367	0.78640777
12	HSP90AA1	56	0.01607905	0.75700935
13	Casp9	49	0.00930122	0.71052632
14	Casp8	50	0.0148875	0.71681416
15	Bcl2l1	50	0.0089411	0.71681416

Abbreviations: Casp3, Caspase3; TP53, tumor protein p53; Bcl2, B-cell lymphoma 2; TLR4, toll-like receptor-4; STAT3, signal transducer and activator of transcription 3; STAT1, signal transducer and activator of transcription 1; NF-κB p65, nuclear factor kappa-B p65; MCL1, myeloid cell leukemia-1; IL-1β, Interleukin-1β; HSP90AA1, heat Shock Protein 90 Alpha Family Class A Member 1; Casp9, Caspase 9; Casp8, Caspase8; Bcl2l1, B-cell lymphoma 2 like 1.

endothelial barrier dysfunction. Consequently, we needed to further validate whether DCHD can be used as a therapeutic treatment for SALI by modulating the PI3K/AKT/NF-κB pathway, which is involved in anti-PANoptosis (Figure 4G).

Molecular Docking Analysis

Based on HPLC-MS and network pharmacology analyses, baicalin, paeoniforin, and saikosaponin A were identified as the main active components of DCHD. Hence, we conducted a molecular docking analysis using the main components (Baicalin, Paeoniforin, and SaikosaponinA) and three hub genes (Casp3, Bcl2, and Casp8). We found that their binding energies were all <-6.00 kcal/mol, indicating good binding ability of the major components and hub genes (Figure 5A–I). Detailed binding affinity results are presented in Table 3. These results confirmed that baicalin, paeoniforin, and saikosaponin A directly targeted Casp3, Bcl2, and Casp8.

DCHD Alleviates Sepsis-Induced Lung Histopathological Injury, Inflammation, and Oxidative Stress

To investigate the protective effects of DCHD against CLP-induced SALI, we initially evaluated pathological changes in lung tissues using hematoxylin and eosin (H&E) staining. Compared with the sham group, the lung sections showed a clear alveolar structure without edema or inflammatory infiltration, whereas the CLP group showed infiltration of inflammatory cells, alveolar congestion, interstitial edema, and alveolar septal thickening. However, DHCH treatment ameliorated these pathological injuries (Figure 6A and B). To further explore the impact of DCHD on pro-inflammatory factors, mRNA expression levels of TNF-α, IL-6, and IL-1β in lung tissues were determined by qRT-PCR. The mRNA expression levels of IL-6, TNF-α, and IL-1β in the CLP group were significantly higher than those in the sham group, and DHCH administration dramatically reduced their expression (Figure 7A–C). Oxidative stress is of great importance in the development of pulmonary inflammatory diseases, and we measured the levels of SOD, MDA, and CAT in the lung tissues. As expected, CAT and SOD levels were remarkably decreased in the model group, whereas MDA expression was significantly elevated, and DCHD treatment significantly improved these levels (Figure 7D–F).

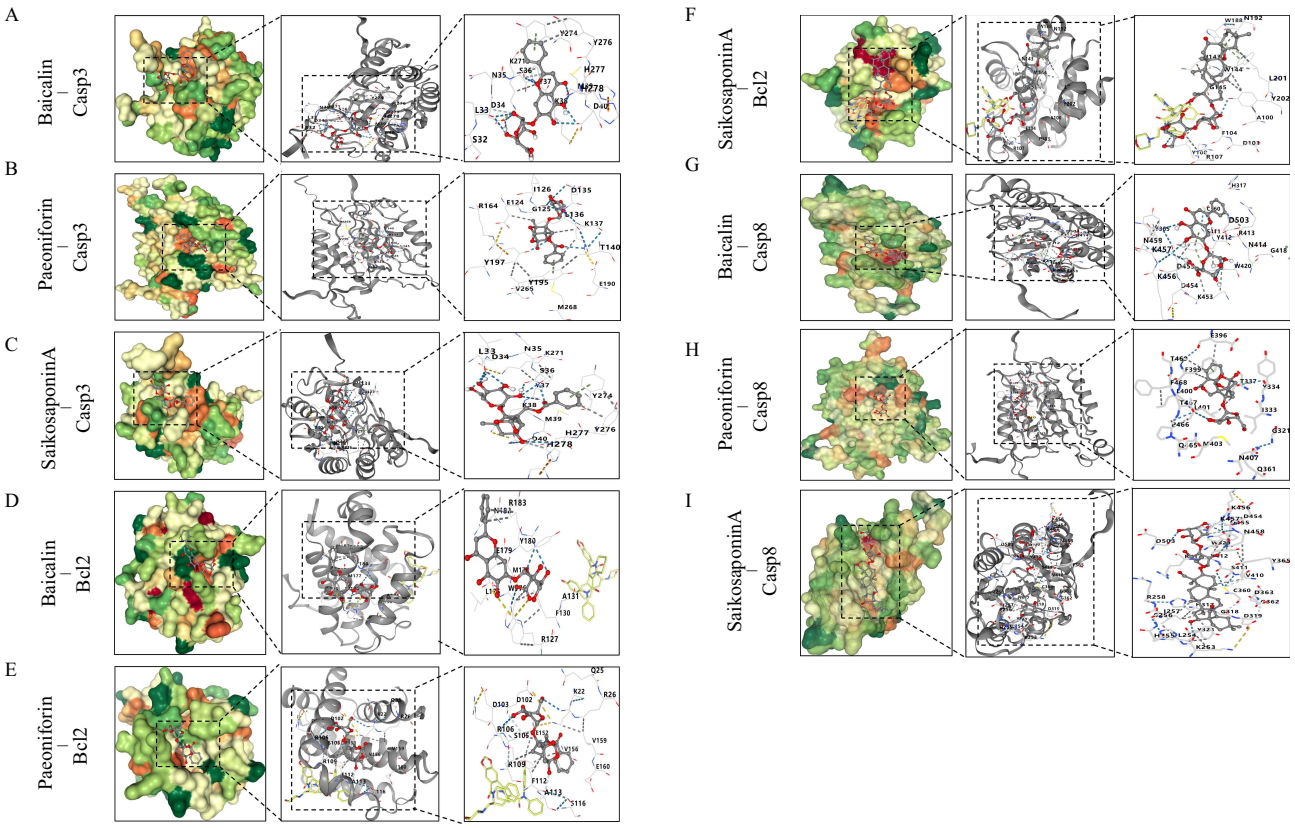

Figure 5 Molecular docking analysis. (**A**) Baicalin-Casp3. (**B**) Paeoniforin-Casp3. (**C**) SaikosaponinA-Casp3. (**D**) Baicalin-Bcl2. (**E**) Paeoniforin-Bcl2. (**F**) SaikosaponinA-Bcl2. (**G**) Baicalin-Casp8. (**H**) Paeoniforin-Casp8. (**I**) SaikosaponinA-Casp8.

Effect of DCHD-DS on Cell Morphology and Pro-Inflammatory Factors in LPS-Induced RAW 264.7 Macrophages

To determine the effects of DCHD-DS on cell morphology and pro-inflammatory factor expression in LPS-induced RAW 264.7 cells. At first, we observed the cell morphology of RAW 264.7, under a light microscope, and found that the cells in the control group showed round or oval shapes with intact cell bodies and no vacuolar appearance. The cells in the model group had obvious tentacles and vacuoles in their bodies. In contrast, the tentacles were reduced and the morphology was close to an oval shape after treatment with DCHD-DS (Figure 8A). We measured the mRNA expression levels of TNF-α, IL-6, and IL-1β in RAW 264.7 cells to further demonstrate the effect of DCHD-DS on pro-inflammatory factors. The results indicated that the mRNA expression levels of TNF-α, IL-6, and IL-1β in the model group was significantly increased compared to the control group in RAW 264.7 cells, and the levels of them were markedly decreased after intervention with DCHD-DS (Figure 8B–D). Furthermore, Western blot assays indicated that IL-6 and TNF-α levels increased in the model group, but decreased in a dose-dependent manner after DCHD intervention (Figure 8E–G). Overall, DCHD-DS alleviated the inflammatory response in the LPS-induced RAW 264.7.

Table 3 The Detailed Results of Binding Affinity Between Hub Genes and the Main Components of DCHD

	Molecular Name	PubChem CID	Hub Genes Docking Score (kcal/mol)		
			Casp3 PDB ID (2j32)	Bcl2 PDB ID (6gl8)	Casp8 PDB ID (4jj7)
Main components	Baicalin	64982	−8.1	−6.5	−7.8
	Paeoniforin	442534	−7.1	−7.1	−7.3
	SaikosaponinA	167928	−7.1	−8	−9.7

Abbreviations: Casp3, Caspase3; Bcl2, B-cell lymphoma 2; Casp8, Caspase8.

https://doi.org/10.2147/DDDT.S495225

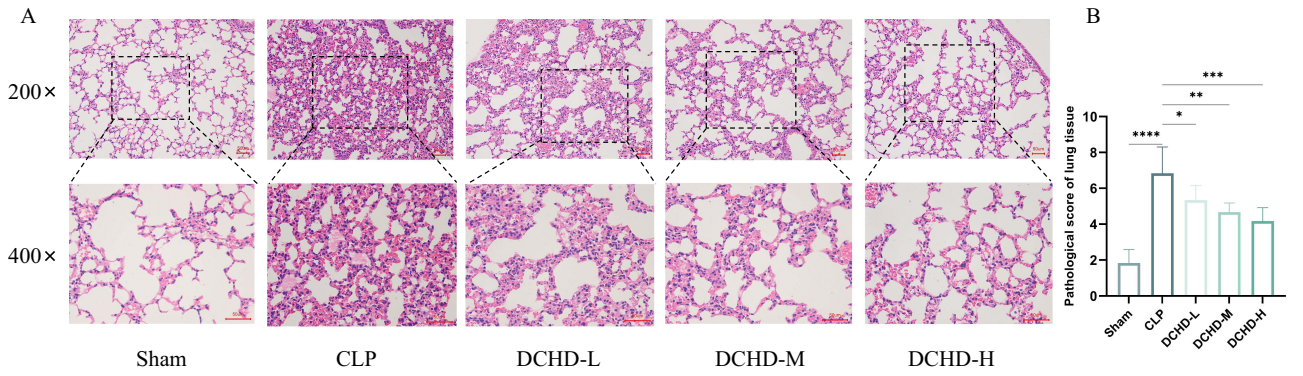

Figure 6 DCHD reduced sepsis-induced acute lung injury by H&E staining. (**A**) Detection of pathological changes in lung tissue by H&E staining (n=6) (scare bar=50 μm). (**B**) The lung injury score (n=6). Date are presented as the mean ± SD. *p < 0.05, **p < 0.01, ***p < 0.001, and ****p < 0.0001 vs CLP group.

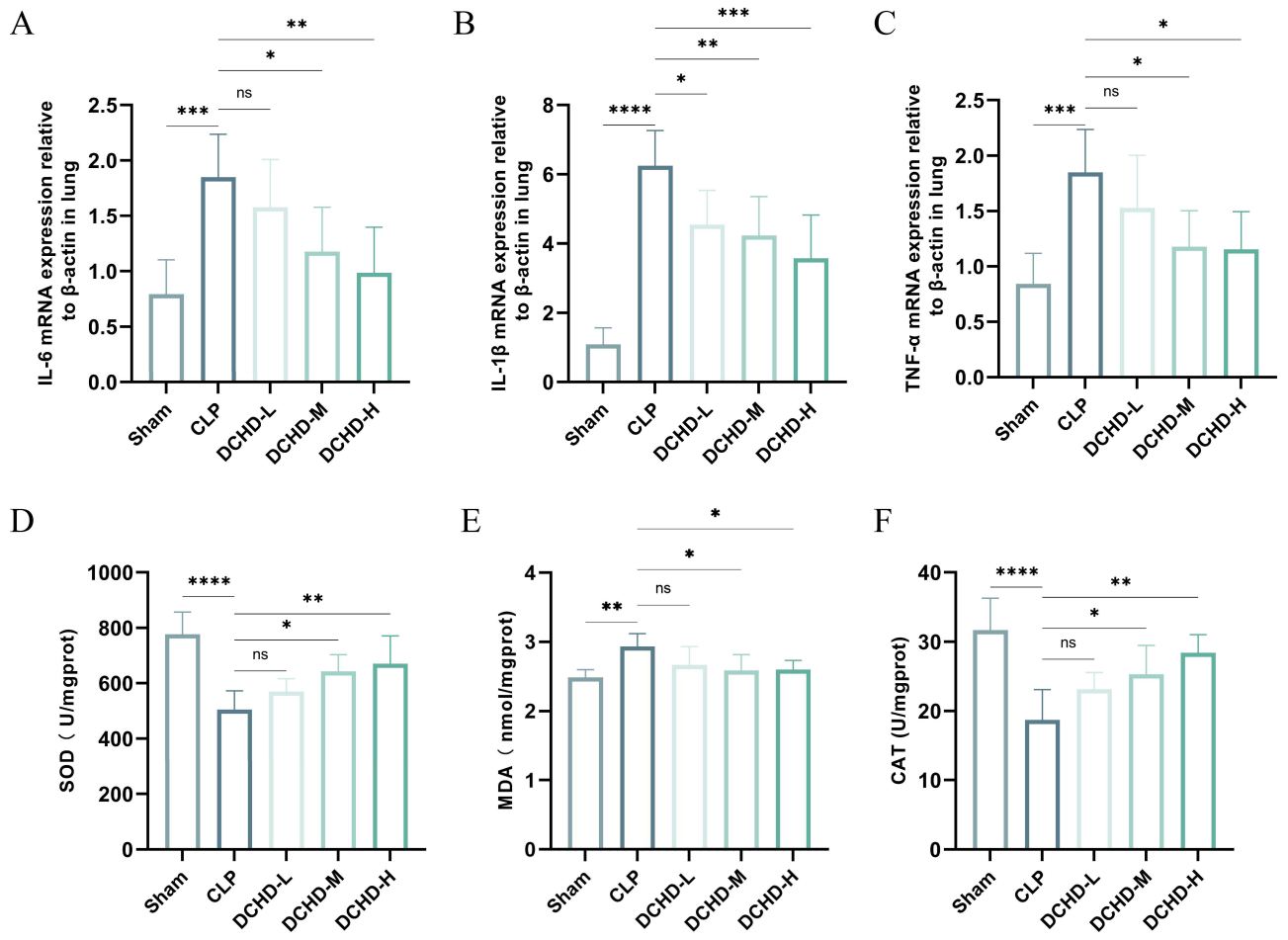

Figure 7 DCHD alleviated ameliorated inflammation response and oxidative stress in mice with SALI. Relative mRNA expression levels of (**A**) IL-6, (**B**) TNF-α, and (**C**) IL-1β in lung tissues (n=6). (**D**) SOD, (**E**) MDA, and (**F**) CAT levels in lung tissues (n=5-6). Date are presented as the mean ± SD, ns = no significance, *p < 0.05, **p < 0.01, ***p < 0.001, and ****p < 0.0001 vs CLP group.

DCHD-DS Suppressed p65 Nuclear Translocation in LPS-Induced RAW 264.7 Macrophages

Since nuclear translocation of the p65 protein is one of the main modes of activation of the NF-κB signaling pathway, we employed immunofluorescence staining and Western blot assays to investigate the effect of DCHD-DS on p65 nuclear translocation in LPS-induced RAW 264.7 macrophages. We observed an increased P65 nucleus translocation in the

 https://doi.org/10.2147/DDDT.S495225

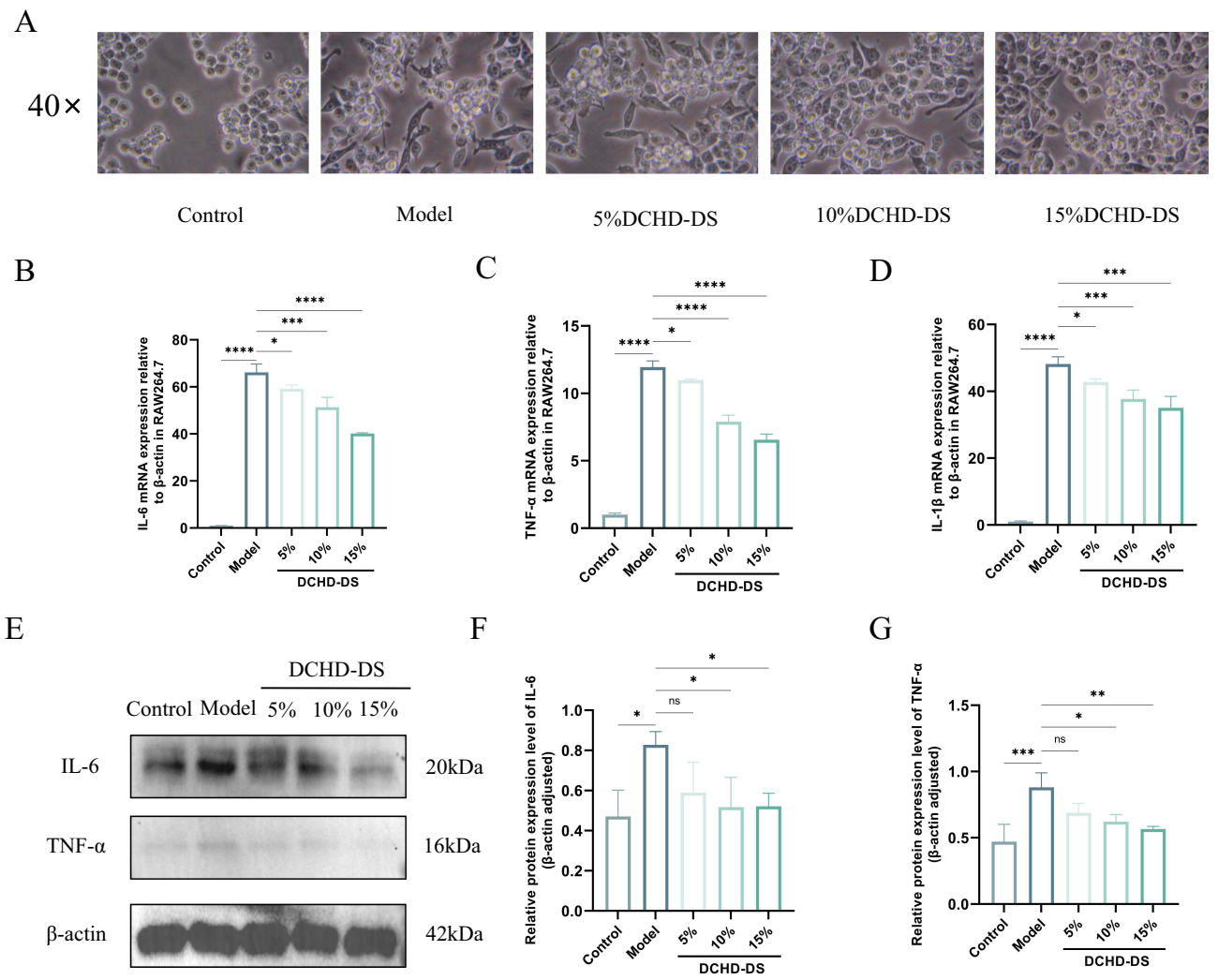

Figure 8 DCHD-DS improved cell morphology and inflammatory response in LPS-induced RAW 264.7 macrophages. (**A**) Morphological observation of LPS-induced RAW 264.7 macrophages treated with different concentrations of DCHD-DS. (**B**–**D**) Relative mRNA expression levels of IL-6, TNF-α, and IL-1β in RAW 264.7 macrophages (n=5). (**E**–**G**) Analysis and quantification of IL-6 and TNF-α expression using Western blotting (n=5). Date are presented as the mean ± SD, ns = no significance, *p < 0.05, **p < 0.01, ***p < 0.001, and ****p < 0.0001 vs model group.

model group. In contrast, DCHD-DS significantly inhibited p65 subunit translocation into the nucleus, resulting in decreased nuclear accumulation of p65 (Figure 9A–C). Furthermore, the results of Western blotting and quantification analyses revealed that the relative protein expression of p-NF-κB p65 was significantly increased in the model group compared to that in the control group, while DCHD-DS effectively reversed the levels of p-NF-κB p65 (Figure 9D–F).

DCHD Inhibited PANoptosis by Regulating PI3K/AKT/NF-κB Signaling Pathway in LPS-Induced RAW 264.7 Macrophages

The PI3K/AKT/NF-κB signaling pathway may be the crucial pathway of DCHD against SALI by inhibiting PANoptosis. According to our previous network pharmacology analysis, we used Western blot assays to verify the results. Our findings indicated that LPS stimulation caused a dramatic increase in the protein expression levels of TLR4, Myd88, p-IκBα, p-PI3K, p-AKT, while Bcl2 was notably downregulated and DCHD-DS reversed these changes (Figure 10A–G). These results confirm that DCHD can alleviate SALI by inhibiting PANoptosis, which is involved in the PI3K/AKT/NF-κB signaling pathway.

https://doi.org/10.2147/DDDT.S495225

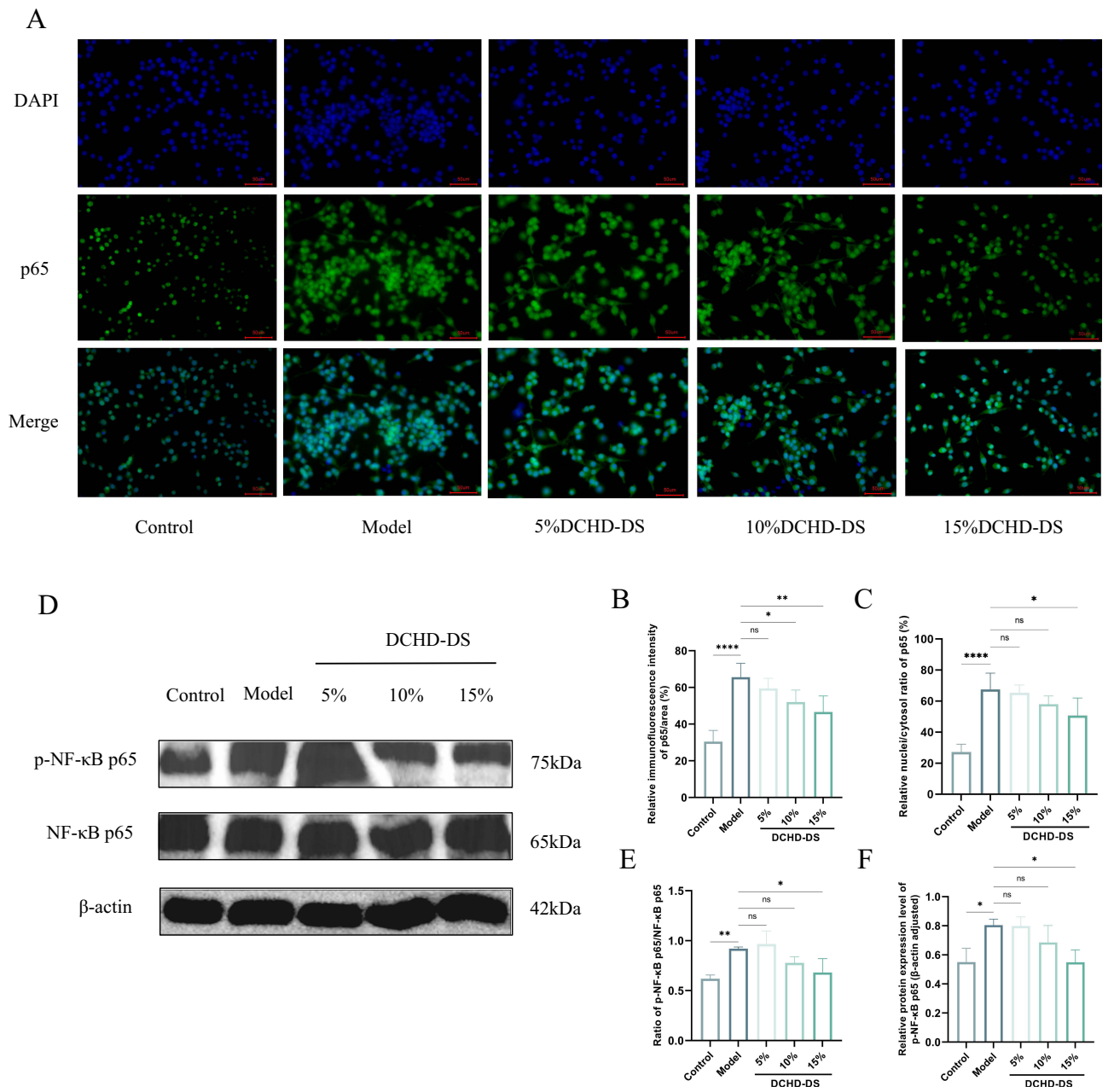

Figure 9 DCHD-DS suppressed p65 nuclear translocation in LPS-induced RAW 264.7 macrophages. (**A**) p65 nuclear translocation was observed by immunofluorescence assay (scare bar=50 μm). (**B** and **C**) p65 immunofluorescence quantitative analysis by the ImageJ software (n=5). (**D**–**F**) Analysis and quantification of p-p65 expression using Western blotting (n=5). Date are presented as the mean ± SD, ns = no significance, *p < 0.05, **p < 0.01, and ****p < 0.0001 vs model group.

Discussion

Sepsis is a leading cause of death in intensive care unit (ICU) patients, and ALI is a common complication of sepsis that often causes life-threatening multiple organ dysfunction syndrome. Despite the high morbidity and mortality associated with SALI in clinical practice, its pathogenesis is still under investigation and effective treatment strategies are still lacking in the clinic.[7,42] An increasing number of studies have shown that TCM can improve SALI by reducing inflammation,[17] inhibiting oxidative stress,[18] regulating gut microbiota,[20] modulating programmed cell death.[43] As a new inflammatory programmed cell death mode, PANoptosis has the key features of pyroptosis, apoptosis, and necroptosis, which are involved in the development of inflammatory diseases.[44] Recent studies have found that

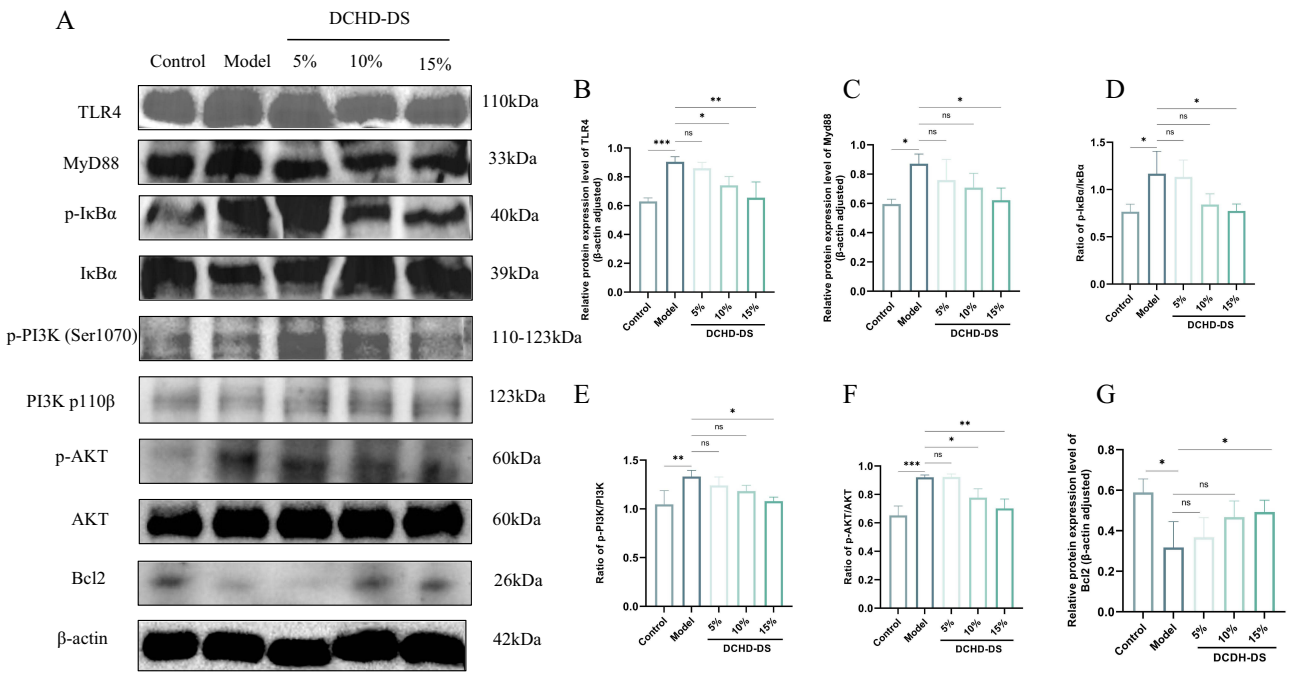

Figure 10 DCHD inhibited PANoptosis by regulating the PI3K/AKT/NF-κB signaling pathway. (**A**–**G**) Analysis and quantification of TLR4, Myd88, p-IκBα, p-PI3K, p-AKT, and Bcl2 expression using Western blotting (n=5). Date are presented as the mean ± SD, ns = no significance, *p < 0.05, **p < 0.01, and ***p < 0.001 vs model group.

Xiaochaihu decoction downregulates genes associated with PANoptosis thereby alleviating sepsis-induced cardiomyopathy, and Dachengqi decoction could inhibit the expression levels of PANoptosis-related proteins of ZBP1 and RIPK1 to alleviate LPS-induced acute lung injury.[45,46] However, the role of PANoptosis in the pathogenesis of SALI remains unclear; therefore, we integrated network pharmacology, bioinformatics, and experimental validation to investigate the mechanisms by which DCHD protects against SALI through anti-PANoptosis.

DCHD is a classic formula that is widely used in clinical practice for the treatment of respiratory, hepatobiliary, and gastrointestinal disorders. Paeoniforin, baicalin, saikosaponin A, kaempferol, and quercetin may be the key components of DCHD based on HPLC-MS and network pharmacology analysis. Previous research has found that Saikosaponin A may protect against sepsis by attenuating the release of inflammatory factors through inhibition of the NOD2/NF-κB signaling pathway.[47] Accumulating evidence has confirmed that baicalin can reduce neutrophil infiltration, the release of pro-inflammatory cytokines, and lymphocyte apoptosis to alleviate sepsis.[48,49] Kaempferol has been reported to protect the lung endothelial cell barrier, suppress inflammatory responses, and reduce lung tissue damage in sepsis model.[50,51] Noticeably, quercetin could reduce inflammation and oxidative stress to alleviate SALI according to the publishes research.[52] These findings imply that DCHD may play a therapeutic role in SALI through multicomponent, multitarget interactions.

ALI and ARDS are commonly characterized by inflammatory cell infiltration, cytokine storms, increased pulmonary capillary permeability, and pulmonary interstitial oedema.[53] During the pathogenesis of SALI, large amounts of inflammatory factors are released, activating intracellular signaling pathways and causing a cytokine storm that destroys lung microvascular endothelial cells and lung epithelial cells possibly causing alveolar epithelial cell PANoptosis.[15,54] Accordingly, CLP was employed to construct an in vivo septic lung injury mouse model in our study in vivo, which is the closest model to human septic patients and is considered the gold standard for sepsis research.[55] Interestingly, our study found that DCHD effectively reduced the infiltration of inflammatory cells, the thickness of the alveolar wall, and interstitial edema. In addition, it is also found that DCHD could decrease the mRNA expression levels of TNF-α, IL-6, and IL-1β in lung tissues, and inhibit oxidative stress. Together, these findings indicate that DCHD plays a protective role in the sepsis-induced ALI model through anti-inflammatory effects and inhibition of oxidative stress.

https://doi.org/10.2147/DDDT.S495225

We used a network pharmacology approach to elucidate the specific mechanisms of action of DCHD against SALI via anti-PANoptosis. Network pharmacology analysis can systematically elaborate on the complex network relationships between drugs, components, target genes, and disease.[56] Fifteen hub genes were identified: Casp3, TP53, Bcl2, TLR4, STAT3, STAT1, NF-κB p65, p50, MCL1, JUN, IL-1β, HSP90AA1, Casp9, Casp8, and Bcl2l1. Notably, Casp3, Casp8, and Casp9 are essential for controlling apoptosis, and Casp8 is considered a molecular switch for apoptosis, necroptosis and pyroptosis.[57,58] Breviscapine targets Casp8 to control neutrophil apoptosis and inflammation, which alleviates SALI in a CLP-induced sepsis mouse model.[59] Moreover, as a key factor in controlling the inflammatory response, the transcription factor NF-κB is often activated by TLR, and activation of NF-κB signaling recruits inflammatory cells by regulating the expression of various inflammatory factors and producing a substantial amount of inflammatory mediators such as IL-Iβ.[60] STAT1 and STAT3 are recognized as potential regulatory targets for treating sepsis and are strongly linked to the production of pro-inflammatory factors. Inhibition of STAT1 and STAT3 activation in macrophages and monocytes effectively improves the pulmonary inflammatory response to ALI induced by LPS.[61–63] Of note, Bcl2, Bcl2l1, and MCL1 are anti-apoptotic members of the Bcl2 family, and regulating their expression can effectively inhibit sepsis-induced exhaustion of dendritic cells, macrophages,[64] and apoptosis of neutrophils.[65] HSP90AA1 is one of the most important heat shock proteins in the HSP90 family, and cardiac troponin has been reported to mitigate the development of myocardial Casp3 activation and apoptosis in septic mice by triggering the HSP90/AKT pathway.[66] As can be observed, the above genes are intimately linked to necroptosis, pyroptosis, and apoptosis that are directly linked to the onset and progression of sepsis.

GO and KEGG pathway enrichment analysis identified crucial biological processes and molecular pathways of DCHD against SALI via anti-PANoptosis. We found that apoptosis, TNF signaling pathway, C-type lectin receptor signaling pathway, AGE-RAGE signaling pathway in diabetic complications, PI3K-AKT signaling pathway, Necroptosis, and Toll-like receptor signaling pathway were the most significantly enriched pathways. Previous studies have revealed that the PI3K/AKT signaling pathway has a broad relationship with autophagy, apoptosis, inflammatory response, and oxidative stress.[67,68] Moreover, *Rhodiola rosea L.*,[69] ginsenoside Rg1,[70] and andrographolide[71] have been shown to ameliorate SALI by regulating the PI3K/AKT pathway. Notably, we found that the PI3K/AKT/NF-κB signaling pathway includes core genes within these pathways in our research, highlighting the critical role of the PI3K/AKT/NF-κB signaling pathway in DCHD against SALI. To further verify these findings, we employed LPS-stimulated RAW 264.7 macrophages to construct an sepsis-induced ALI cell model in vitro.[17]

As the core phagocytes in the body's immune system, macrophages under the action of different stimuli will appear in M1 and M2 polarization states. Maintaining the balance of M1/M2 macrophages is an important means of maintaining homeostasis in the body.[72] Disruption of the dynamic balance between M1/M2 macrophages induces the development of SALI and exacerbates its progression.[73] LPS-induced RAW264.7 macrophages inflammation model is now widely used in the study of inflammatory response. Therefore, we used DCHD-DS to act on LPS-induced RAW 264.7 macrophages, the result showed that DCHD-DS reduced the cellular pseudopodia of LPS-stimulated RAW 264.7 macrophages and gradually restored their normal morphology. According to the qRT-PCR data, DCHD-DS reduced the release of inflammatory factors and improved the pro-inflammatory environment. P65 is then activated and translocated to the nucleus when released from the inhibitory protein IκBα cytoplasmic lysosome.[74] We observed that DCHD-DS significantly p65 the nuclear translocation. Meanwhile, Western Blotting analysis revealed that LPS could upregulate TLR4, Myd88, and p-IκBα, p-PI3K, p-AKT proteins, and downregulate Bcl2 protein in RAW 264.7 macrophages. Following DCHD-DS intervention, these proteins' expression was markedly reversed, indicating that DCHD-DS effectively inhibited the PI3K/AKT/NF-κB signaling pathway in LPS-induced RAW 264.7 macrophages.

However, some shortcomings can be addressed in order to enhance our research. First, there are some limitations in constructing a sepsis mouse model using CLP. Because it is difficult to guarantee the consistency of the model, we can only use one researcher to operate and maintain the ligation position consistently to reduce the error. Second, a larger sample size is required to reduce experimental errors. Third, further clinical trials are necessary to verify the clinical efficacy and safety of DCHD in the treatment of SALI. Finally, in-depth pharmacokinetic and molecular mechanisms studies are required to elucidate the DCHD against SALI via anti-PANoptosis in vivo.

Conclusion

In conclusion, DCHD is a famous and ancient TCM formula, which is now widely used in clinical practice for the treatment of SALI due to its safety and effectiveness. PANoptosis is a novel indicator of programmed cell death that is closely associated with the development of SALI. Herein, DCHD exerted a therapeutic effect on SALI by reducing the inflammatory response and oxidative stress, and regulating the PI3K/AKT/NF-κB signaling pathway, thereby inhibiting PANoptosis. Our research demonstrates that DCHD can be used as a complementary alternative therapy for the clinical treatment of SALI, and deserves further intensive investigation.

Abbreviations

ALI, acute lung injury; ARDS, acute respiratory distress syndrome; SALI, sepsis-induced acute lung injury; TNF, tumor necrosis factor; IL, interleukin; FAS, factor-related apoptosis; CD, cluster of differentiation; TCM, traditional Chinese medicine; JAK, janus kinase; STAT, signal transducer and activator of transcription; MAPK, mitogen-activated protein kinase; ANOVA, analysis of variance; TLR4, toll-like receptor-4; MyD88, myeloiddifferentiationfactor88; IκBα, inhibitor kappa B alpha; NF-κB, nuclear factor kappa-B; PI3K, Phosphoinositide 3-kinase; AKT, protein kinase B; DCHD, Da Chaihu decoction; SOD, superoxide dismutase; MDA, malondialdehyde; CAT, catalase; BSA, bovine serum albumin; DMEM, Dulbecco's modified Eagle's medium; FBS, fetal bovine serum; P/S, Penicillin-streptomycin; HPLC-MS, high performance liquid chromatography combined with mass spectrometry; TCMSP, Traditional Chinese Medicine Systems Pharmacology Database; ADME, absorption, distribution, metabolism, excretion; GEO, Gene Expression Omnibus; DEGs, differentially expressed genes; MCC, Maximal Clique Centrality; PPI, protein-protein interaction; GO, Gene Ontology; KEGG, Kyoto Encyclopedia of Genes and Genomes; BP, biological pathways; CC, cellular components; MF, molecular functions; BCL2, B-cell lymphoma 2; CASP, Caspase; TP53; Cellular tumor antigen p53; STAT, signal transducer and activator of transcription; MCL1, myeloid cell leukemia-1; HSP, heat shock protein; H&E, hematoxylin and eosin; qRT-PCR, quantitative real-time PCR.

Credit Author Statement

All authors made a significant contribution to the work reported, whether that is in the conception, study design, execution, acquisition of data, analysis and interpretation, or in all these areas; took part in drafting, revising or critically reviewing the article; gave final approval of the version to be published; have agreed on the journal to which the article has been submitted; and agree to be accountable for all aspects of the work.

Funding

This study was supported by the National Natural Science Foundation of China (grant number: 82374216).

Disclosure

The authors declare no conflict of interest.

References

1. Angus DC, van der Poll T. Severe sepsis and septic shock. *N Engl J Med*. 2013;369:840–851. doi:10.1056/NEJMra1208623
2. Singer M, Deutschman CS, Seymour CW, et al. The third international consensus definitions for sepsis and septic shock (sepsis-3). *JAMA*. 2016;315:801–810. doi:10.1001/jama.2016.0287
3. Vandini S, Bottau P, Faldella G, Lanari M. Immunological, viral, environmental, and individual factors modulating lung immune response to respiratory syncytial virus. *Biomed Res Int*. 2015;2015:875723. doi:10.1155/2015/875723
4. Sinha P, Meyer NJ, Calfee CS. Biological phenotyping in sepsis and acute respiratory distress syndrome. *Annu Rev Med*. 2023;74:457–471. doi:10.1146/annurev-med-043021-014005
5. Esposito S, De Simone G, Boccia G, De Caro F, Pagliano P. Sepsis and septic shock: new definitions, new diagnostic and therapeutic approaches. *J Glob Antimicrob Resist*. 2017;10:204–212. doi:10.1016/j.jgar.2017.06.013
6. Xie J, Wang H, Kang Y, et al. The epidemiology of sepsis in Chinese icus: a national cross-sectional survey. *Crit Care Med*. 2020;48:e209–e218. doi:10.1097/CCM.0000000000004155
7. Kumar V. Pulmonary innate immune response determines the outcome of inflammation during pneumonia and sepsis-associated acute lung injury. *Front Immunol*. 2020;11:1722. doi:10.3389/fimmu.2020.01722
8. Thompson BT, Chambers RC, Liu KD. Acute respiratory distress syndrome. *N Engl J Med*. 2017;377:562–572. doi:10.1056/NEJMra1608077

9. Li W, Li D, Chen Y, et al. Classic signaling pathways in alveolar injury and repair involved in sepsis-induced ali/ards: new research progress and prospect. *Dis Markers*. 2022;2022:6362344. doi:10.1155/2022/6362344
10. Lelubre C, Vincent JL. Mechanisms and treatment of organ failure in sepsis. *Nat Rev Nephrol*. 2018;14:417–427. doi:10.1038/s41581-018-0005-7
11. Wang Y, Kanneganti TD. From pyroptosis, apoptosis and necroptosis to panoptosis: a mechanistic compendium of programmed cell death pathways. *Comput Struct Biotechnol J*. 2021;19:4641–4657. doi:10.1016/j.csbj.2021.07.038
12. Sun X, Yang Y, Meng X, Li J, Liu X, Liu H. Panoptosis: mechanisms, biology, and role in disease. *Immunol Rev*. 2024;321:246–262. doi:10.1111/imr.13279
13. Zhu P, Ke ZR, Chen JX, Li SJ, Ma TL, Fan XL. Advances in mechanism and regulation of panoptosis: prospects in disease treatment. *Front Immunol*. 2023;14:1120034. doi:10.3389/fimmu.2023.1120034
14. He YQ, Deng JL, Zhou CC, et al. Ursodeoxycholic acid alleviates sepsis-induced lung injury by blocking panoptosis via sting pathway. *Int Immunopharmacol*. 2023;125:111161. doi:10.1016/j.intimp.2023.111161
15. Cui Y, Wang X, Lin F, et al. Mir-29a-3p improves acute lung injury by reducing alveolar epithelial cell panoptosis. *Aging Dis*. 2022;13:899–909. doi:10.14336/AD.2021.1023
16. Yang R, Yang H, Wei J, et al. Mechanisms underlying the effects of lianhua qingwen on sepsis-induced acute lung injury: a network pharmacology approach. *Front Pharmacol*. 2021;12:717652. doi:10.3389/fphar.2021.717652
17. Xie L, Zhang G, Wu Y, et al. Protective effects of wenqingyin on sepsis-induced acute lung injury through regulation of the receptor for advanced glycation end products pathway. *Phytomedicine*. 2024;129:155654. doi:10.1016/j.phymed.2024.155654
18. Li Z, Yu Y, Bu Y, et al. Qishenyiqi pills preserve endothelial barrier integrity to mitigate sepsis-induced acute lung injury by inhibiting ferroptosis. *J Ethnopharmacol*. 2024;322:117610. doi:10.1016/j.jep.2023.117610
19. Zhang SK, Zhuo YZ, Li CX, Yang L, Gao HW, Wang XM. Xuebijing injection and resolvin d1 synergize regulate leukocyte adhesion and improve survival rate in mice with sepsis-induced lung injury. *Chin J Integr Med*. 2018;24:272–277. doi:10.1007/s11655-017-2959-x
20. Bao K, Wang M, Liu L, et al. Jinhong decoction protects sepsis-associated acute lung injury by reducing intestinal bacterial translocation and improving gut microbial homeostasis. *Front Pharmacol*. 2023;14:1079482. doi:10.3389/fphar.2023.1079482
21. Bi S, Liu Y, Lv T, et al. Preliminary exploration of method for screening efficacy markers compatibility in tcm prescriptions based on q-markers: anti-inflammatory activity of Dachaihu decoction as an example. *J Ethnopharmacol*. 2023;312:116539. doi:10.1016/j.jep.2023.116539
22. Cui H, Li Y, Wang Y, et al. Da-chai-hu decoction ameliorates high fat diet-induced nonalcoholic fatty liver disease through remodeling the gut microbiota and modulating the serum metabolism. *Front Pharmacol*. 2020;11:584090. doi:10.3389/fphar.2020.584090
23. Duan LF, Xu XF, Zhu LJ, et al. Dachaihu decoction ameliorates pancreatic fibrosis by inhibiting macrophage infiltration in chronic pancreatitis. *World J Gastroenterol*. 2017;23:7242–7252. doi:10.3748/wjg.v23.i40.7242
24. Zeng Y, Li N, Zheng Z, et al. Screening of key biomarkers and immune infiltration in pulmonary arterial hypertension via integrated bioinformatics analysis. *Bioengineered*. 2021;12:2576–2591. doi:10.1080/21655979.2021.1936816
25. Huang N, Wei Y, Liu M, et al. Dachaihu decoction ameliorates septic intestinal injury via modulating the gut microbiota and glutathione metabolism as revealed by multi-omics. *J Ethnopharmacol*. 2023;312:116505. doi:10.1016/j.jep.2023.116505
26. Sun L, Yang Z, Zhao W, et al. Integrated lipidomics, transcriptomics and network pharmacology analysis to reveal the mechanisms of danggui buxue decoction in the treatment of diabetic nephropathy in type 2 diabetes mellitus. *J Ethnopharmacol*. 2022;283:114699. doi:10.1016/j.jep.2021.114699
27. Ru J, Li P, Wang J, et al. Tcmsp: a database of systems pharmacology for drug discovery from herbal medicines. *J Cheminform*. 2014;6:13. doi:10.1186/1758-2946-6-13
28. Wang S, Wang H, Lu Y. Tianfoshen oral liquid: a CFDA approved clinical traditional Chinese medicine, normalizes major cellular pathways disordered during colorectal carcinogenesis. *Oncotarget*. 2017;8:14549–14569. doi:10.18632/oncotarget.14675
29. Kim S, Chen J, Cheng T, et al. PubChem 2019 update: improved access to chemical data. *Nucleic Acids Res*. 2019;47:D1102–D1109. doi:10.1093/nar/gky1033
30. Daina A, Michielin O, Zoete V. Swisstargetprediction: updated data and new features for efficient prediction of protein targets of small molecules. *Nucleic Acids Res*. 2019;47:W357–W364. doi:10.1093/nar/gkz382
31. Barrett T, Wilhite SE, Ledoux P, et al. NCBI Geo: archive for functional genomics data sets--update. *Nucleic Acids Res*. 2013;41:D991–D995. doi:10.1093/nar/gks1193
32. Yi X, Li J, Zheng X, et al. Construction of panoptosis signature: novel target discovery for prostate cancer immunotherapy. *Mol Ther Nucleic Acids*. 2023;33:376–390. doi:10.1016/j.omtn.2023.07.010
33. Song F, Wang CG, Mao JZ, et al. Panoptosis-based molecular subtyping and hpan-index predicts therapeutic response and survival in hepatocellular carcinoma. *Front Immunol*. 2023;14:1197152. doi:10.3389/fimmu.2023.1197152
34. Bardou P, Mariette J, Escudie F, Djemiel C, Klopp C. Jvenn: an interactive venn diagram viewer. *BMC Bioinformatics*. 2014;15:293. doi:10.1186/1471-2105-15-293
35. Pinzi L, Rastelli G. Molecular docking: shifting paradigms in drug discovery. *Int J Mol Sci*. 2019;20:4331. doi:10.3390/ijms20184331
36. Gaillard T. Evaluation of autodock and autodock vina on the casf-2013 benchmark. *J Chem Inf Model*. 2018;58:1697–1706. doi:10.1021/acs.jcim.8b00312
37. Rittirsch D, Huber-Lang MS, Flierl MA, Ward PA. Immunodesign of experimental sepsis by cecal ligation and puncture. *Nat Protoc*. 2009;4:31–36. doi:10.1038/nprot.2008.214
38. Wang Y, Zhang J, Zhang B, et al. Modified gegen qinlian decoction ameliorated ulcerative colitis by attenuating inflammation and oxidative stress and enhancing intestinal barrier function in vivo and in vitro. *J Ethnopharmacol*. 2023;313:116538. doi:10.1016/j.jep.2023.116538
39. He H, Liu L, Chen Q, et al. Mesenchymal stem cells overexpressing angiotensin-converting enzyme 2 rescue lipopolysaccharide-induced lung injury. *Cell Transplant*. 2015;24:1699–1715. doi:10.3727/096368914X685087
40. Zhang K, Wang ZC, Sun H, Long H, Wang Y. Esculentoside h reduces the panoptosis and protects the blood-brain barrier after cerebral ischemia/reperfusion through the tle1/pi3k/akt signaling pathway. *Exp Neurol*. 2024;379:114850. doi:10.1016/j.expneurol.2024.114850
41. Zhao D, Wu L, Fang X, et al. Copper exposure induces inflammation and panoptosis through the tlr4/nf-kappab signaling pathway, leading to testicular damage and impaired spermatogenesis in Wilson disease. *Chem Biol Interact*. 2024;396:111060. doi:10.1016/j.cbi.2024.111060
42. Huang M, Cai S, Su J. The pathogenesis of sepsis and potential therapeutic targets. *Int J Mol Sci*. 2019;20:5376. doi:10.3390/ijms20215376

43. Hu Y, He S, Xu X, et al. Shenhuangdan decoction alleviates sepsis-induced lung injury through inhibition of gsdmd-mediated pyroptosis. *J Ethnopharmacol*. 2024;318:117047. doi:10.1016/j.jep.2023.117047
44. Christgen S, Zheng M, Kesavardhana S, et al. Identification of the panoptosome: a molecular platform triggering pyroptosis, apoptosis, and necroptosis (panoptosis). *Front Cell Infect Microbiol*. 2020;10:237. doi:10.3389/fcimb.2020.00237
45. Wang Y, Fu X, Shang Z, et al. In vivo and in vitro study on the regulatory mechanism of xiaochaihu decoction on panoptosis in sepsis-induced cardiomyopathy. *J Ethnopharmacol*. 2025;336:118740. doi:10.1016/j.jep.2024.118740
46. Zhang M, Shang L, Zhou F, et al. Dachengqi decoction dispensing granule ameliorates lps-induced acute lung injury by inhibiting panoptosis in vivo and in vitro. *J Ethnopharmacol*. 2025;336:118699. doi:10.1016/j.jep.2024.118699
47. Zhao H, Li S, Zhang H, Wang G, Xu G, Zhang H. Saikosaponin a protects against experimental sepsis via inhibition of nod2-mediated nf-kappab activation. *Exp Ther Med*. 2015;10:823–827. doi:10.3892/etm.2015.2558
48. Zhu J, Wang J, Sheng Y, et al. Baicalin improves survival in a murine model of polymicrobial sepsis via suppressing inflammatory response and lymphocyte apoptosis. *PLoS One*. 2012;7:e35523. doi:10.1371/journal.pone.0035523
49. Wang H, Liu D. Baicalin inhibits high-mobility group box 1 release and improves survival in experimental sepsis. *Shock*. 2014;41:324–330. doi:10.1097/SHK.0000000000000122
50. Gao M, Zhu X, Gao X, et al. Kaempferol mitigates sepsis-induced acute lung injury by modulating the sphk1/s1p/s1pr1/mlc2 signaling pathway to restore the integrity of the pulmonary endothelial cell barrier. *Chem Biol Interact*. 2024;398:111085. doi:10.1016/j.cbi.2024.111085
51. Zhu X, Wang X, Ying T, et al. Kaempferol alleviates the inflammatory response and stabilizes the pulmonary vascular endothelial barrier in lps-induced sepsis through regulating the sphk1/s1p signaling pathway. *Chem Biol Interact*. 2022;368:110221. doi:10.1016/j.cbi.2022.110221
52. Gerin F, Sener U, Erman H, et al. The effects of quercetin on acute lung injury and biomarkers of inflammation and oxidative stress in the rat model of sepsis. *Inflammation*. 2016;39:700–705. doi:10.1007/s10753-015-0296-9
53. Matthay MA, Zemans RL, Zimmerman GA, et al. Acute respiratory distress syndrome. *Nat Rev Dis Primers*. 2019;5:18. doi:10.1038/s41572-019-0069-0
54. Zhang X, Zhang Y, Qiao W, Zhang J, Qi Z. Baricitinib, a drug with potential effect to prevent SARS-cov-2 from entering target cells and control cytokine storm induced by covid-19. *Int Immunopharmacol*. 2020;86:106749. doi:10.1016/j.intimp.2020.106749
55. Cai L, Rodgers E, Schoenmann N, Raju RP. Advances in rodent experimental models of sepsis. *Int J Mol Sci*. 2023;24:9578. doi:10.3390/ijms24119578
56. Duan ZL, Wang YJ, Lu ZH, et al. Wumei wan attenuates angiogenesis and inflammation by modulating rage signaling pathway in ibd: network pharmacology analysis and experimental evidence. *Phytomedicine*. 2023;111:154658. doi:10.1016/j.phymed.2023.154658
57. Liamarkopoulos E, Gazouli M, Aravantinos G, et al. Caspase 8 and caspase 9 gene polymorphisms and susceptibility to gastric cancer. *Gastric Cancer*. 2011;14:317–321. doi:10.1007/s10120-011-0045-1
58. Fritsch M, Gunther SD, Schwarzer R, et al. Caspase-8 is the molecular switch for apoptosis, necroptosis and pyroptosis. *Nature*. 2019;575:683–687. doi:10.1038/s41586-019-1770-6
59. Song J, Zhang J, Shi J, Pan X, Mo D. Breviscapine reduces sepsis-induced acute lung injury by targeting casp8 to regulate neutrophil apoptosis and inflammation. *J Inflamm Res*. 2024;17:5161–5176. doi:10.2147/JIR.S446345
60. Verstrepen L, Bekaert T, Chau TL, Tavernier J, Chariot A, Beyaert R. Tlr-4, il-1r and tnf-r signaling to nf-kappab: variations on a common theme. *Cell Mol Life Sci*. 2008;65:2964–2978. doi:10.1007/s00018-008-8064-8
61. Cheng YJ, Tian XL, Zeng YZ, et al. Esculetin protects against early sepsis via attenuating inflammation by inhibiting nf-kappab and stat1/stat3 signaling. *Chin J Nat Med*. 2021;19:432–441. doi:10.1016/S1875-5364(21)60042-0
62. Herzig D, Fang G, Toliver-Kinsky TE, Guo Y, Bohannon J, Sherwood ER. Stat1-deficient mice are resistant to cecal ligation and puncture-induced septic shock. *Shock*. 2012;38:395–402. doi:10.1097/SHK.0b013e318265a2ab
63. Zhao J, Yu H, Liu Y, et al. Protective effect of suppressing stat3 activity in lps-induced acute lung injury. *Am J Physiol Lung Cell Mol Physiol*. 2016;311:L868–L880. doi:10.1152/ajplung.00281.2016
64. Peck-Palmer OM, Unsinger J, Chang KC, et al. Modulation of the bcl-2 family blocks sepsis-induced depletion of dendritic cells and macrophages. *Shock*. 2009;31:359–366. doi:10.1097/SHK.0b013e31818ba2a2
65. Harter L, Mica L, Stocker R, Trentz O, Keel M. Mcl-1 correlates with reduced apoptosis in neutrophils from patients with sepsis. *J Am Coll Surg*. 2003;197:964–973. doi:10.1016/j.jamcollsurg.2003.07.008
66. Li X, Luo R, Jiang R, et al. The role of the hsp90/akt pathway in myocardial calpain-induced caspase-3 activation and apoptosis during sepsis. *BMC Cardiovasc Disord*. 2013;13:8. doi:10.1186/1471-2261-13-8
67. Chen J, Ding W, Zhang Z, et al. Shenfu injection targets the pi3k-akt pathway to regulate autophagy and apoptosis in acute respiratory distress syndrome caused by sepsis. *Phytomedicine*. 2024;129:155627. doi:10.1016/j.phymed.2024.155627
68. Zhong W, Qian K, Xiong J, Ma K, Wang A, Zou Y. Curcumin alleviates lipopolysaccharide induced sepsis and liver failure by suppression of oxidative stress-related inflammation via pi3k/akt and nf-kappab related signaling. *Biomed Pharmacother*. 2016;83:302–313. doi:10.1016/j.biopha.2016.06.036
69. Jiang L, Yang D, Zhang Z, et al. Elucidating the role of rhodiola rosea l. In sepsis-induced acute lung injury via network pharmacology: emphasis on inflammatory response, oxidative stress, and the pi3k-akt pathway. *Pharm Biol*. 2024;62:272–284. doi:10.1080/13880209.2024.2319117
70. Zhong K, Huang Y, Chen R, Pan Q, Li J, Xi X. The protective effect of ginsenoside rg1 against sepsis-induced lung injury through pi3k-akt pathway: insights from molecular dynamics simulation and experimental validation. *Sci Rep*. 2024;14:16071. doi:10.1038/s41598-024-66908-y
71. Qin Y, Li W, Liu J, et al. Andrographolide ameliorates sepsis-induced acute lung injury by promoting autophagy in alveolar macrophages via the rage/pi3k/akt/mtor pathway. *Int Immunopharmacol*. 2024;139:112719. doi:10.1016/j.intimp.2024.112719
72. Ross EA, Devitt A, Johnson JR. Macrophages: the good, the bad, and the gluttony. *Front Immunol*. 2021;12:708186. doi:10.3389/fimmu.2021.708186
73. Wang Z, Wang Z. The role of macrophages polarization in sepsis-induced acute lung injury. *Front Immunol*. 2023;14:1209438. doi:10.3389/fimmu.2023.1209438
74. Mitchell S, Vargas J, Hoffmann A. Signaling via the NFkappaB system. *Wiley Interdiscip Rev Syst Biol Med*. 2016;8:227–241. doi:10.1002/wsbm.1331

Drug Design, Development and Therapy

Dovepress
Taylor & Francis Group

Publish your work in this journal

Drug Design, Development and Therapy is an international, peer-reviewed open-access journal that spans the spectrum of drug design and development through to clinical applications. Clinical outcomes, patient safety, and programs for the development and effective, safe, and sustained use of medicines are a feature of the journal, which has also been accepted for indexing on PubMed Central. The manuscript management system is completely online and includes a very quick and fair peer-review system, which is all easy to use. Visit http://www.dovepress.com/testimonials.php to read real quotes from published authors.

Submit your manuscript here: https://www.dovepress.com/drug-design-development-and-therapy-journal